Ruytenschildt Bridge
Field and laboratory testing

Lantsoght, Eva; Yang, Yuguang; van der Veen, Cor; de Boer, A; Hordijk, Dick

DOI
10.1016/j.engstruct.2016.09.029
Publication date
2016
Document Version
Accepted author manuscript
Published in
Engineering Structures

Elsevier Editorial System(tm) for Engineering Structures
Manuscript Draft

Manuscript Number: ENGSTRUCT-D-16-00450R2

Title: Ruytenschildt Bridge: field and laboratory testing

Article Type: Research Paper

Keywords: Assessment; Beam test; Bending moment capacity; Bond properties; Field test; Plain reinforcement; Shear capacity; Slab bridge.

Corresponding Author: Dr. Eva Lantsoght,

Corresponding Author's Institution: Universidad San Francisco de Quito

First Author: Eva Lantsoght

Order of Authors: Eva Lantsoght; Yuguang Yang; Cor van der Veen; Ane de Boer; Dick Hordijk

Abstract: A large number of existing reinforced concrete solid slab bridges in the Netherlands are found to be insufficient for shear upon assessment. However, research has shown additional sources of capacity in slab bridges, increasing their total capacity. Previous testing was limited to half-scale slab specimens cast in the laboratory. To study the full structural behavior of slab bridges, testing to failure of a bridge is necessary. In August 2014, a bridge was tested to failure in two spans. Afterwards, beams were sawn out of the bridge for experimental work in the laboratory and further study. Though calculations with current design provisions showed that the bridge could fail in shear, the field test showed failure in flexure before shear. The experiments on the beams study the transition from flexural to shear failure and the influence of the type of reinforcement on the capacity. The experimental results were compared to predictions of the capacity for the bridge slab and the sawn beams. These comparisons show that the current methods for rating of existing reinforced concrete slab bridges, leading to a sharper assessment, are conservative. It was also found that the application of plain bars instead of deformed bars does not increase the shear capacity of beams.

Reviewer #1: Paper review

Manuscript Number ENGSTRUCT-D-16-00450R1
Title: Ruytenschildt Bridge: field and laboratory testing
By: Eva O.L. Lantsoght, Yuguang Yang, Cor van der Veen, Ane de Boer, Dick A. Hordijk

General remarks:

General, all reviewer suggestions and comments are well considered in new version of the paper. The revised paper looks quite good. Only the conclusions are too "dry" and an aesthetics (description, dimension lines, dimensions, etc.) of figures should be improved, despite this I recommend to publish this paper in the Engineering Structures. My last comments should be considered by Editor only (without formal re-review).

We've rewritten the conclusions into a text form instead of bullet points, and revised the figures and changed lines and added units where appropriate.

- Few tests to failure on bridges are available in the literature.
- This paper presents the testing to failure in 2 spans of a reinforced concrete slab bridge
- The field test resulted in flexural failures.
- Beams sawn from the bridge were tested in the laboratory.
- The laboratory tests resulted in shear and flexural failures.

Abstract

A large number of existing reinforced concrete solid slab bridges in the Netherlands are found to be insufficient for shear upon assessment. However, research has shown additional sources of capacity in slab bridges, increasing their total capacity. Previous testing was limited to half-scale slab specimens cast in the laboratory. To study the full structural behavior of slab bridges, testing to failure of a bridge is necessary. In August 2014, a bridge was tested to failure in two spans. Afterwards, beams were sawn out of the bridge for experimental work in the laboratory and further study. Though calculations with current design provisions showed that the bridge could fail in shear, the field test showed failure in flexure before shear. The experiments on the beams study the transition from flexural to shear failure and the influence of the type of reinforcement on the capacity. The experimental results were compared to predictions of the capacity for the bridge slab and the sawn beams. These comparisons show that the current methods for rating of existing reinforced concrete slab bridges, leading to a sharper assessment, are conservative. It was also found that the application of plain bars instead of deformed bars does not increase the shear capacity of beams.

Ruytenschildt Bridge: field and laboratory testing

Eva O.L. Lantsoght[a,b] (E.O.L.Lantsoght@tudelft.nl Tel: +593 2 297-1700 ext. 1186 Corresponding Author), Yuguang Yang[b] (Yuguang.Yang@tudelft.nl), Cor van der Veen[b] (C.vanderveen@tudelft.nl), Ane de Boer[c] (ane.de.boer@rws.nl), Dick A. Hordijk (D.A.Hordijk@tudelft.nl)

[a]Universidad San Francisco de Quito, Politecnico, Diego de Robles y Vía Interoceánica, Quito, Ecuador

[b]Delft University of Technology, Concrete Structures, Stevinweg 1, 2628 CN Delft, The Netherlands

[c]Ministry of Infrastructure and the Environment, Griffioenlaan 2, 3526 LA Utrecht, The Netherlands

Abstract

A large number of existing reinforced concrete solid slab bridges in the Netherlands are found to be insufficient for shear upon assessment. However, research has shown additional sources of capacity in slab bridges, increasing their total capacity. Previous testing was limited to half-scale slab specimens cast in the laboratory. To study the full structural behavior of slab bridges, testing to failure of a bridge is necessary. In August 2014, a bridge was tested to failure in two spans. Afterwards, beams were sawn out of the bridge for experimental work in the laboratory and further study. Though calculations with current design provisions showed that the bridge could fail in shear, the field test showed failure in flexure before shear. The experiments on the beams study the transition from flexural to shear failure and the influence of the type of reinforcement on the capacity. The experimental results were compared to predictions of the capacity for the bridge slab and the sawn beams. These comparisons show that the current methods for rating of existing reinforced concrete slab bridges, leading to a sharper assessment, are conservative. It was also found that the application of plain bars instead of deformed bars does not increase the shear capacity of beams.

Keywords

Assessment; Beam test; Bending moment capacity; Bond properties; Field test; Plain reinforcement; Shear capacity; Slab bridge.

1. Introduction

1.1. Existing slab bridges in The Netherlands and code changes

The majority of the bridges in The Netherlands were built during the years following the Second World War. These bridges were designed for the live loads of that era, which are considerably lower than the current live loads (see NEN-EN 1991-2+NA:2011 [1]). In NEN-EN 1992-1-1:2005 [2] the shear capacity of a cross-section is also lower than in the previously used NEN 6720:1995 [3].

The shear capacity for an element without axial load or prestressing and without shear reinforcement, according to NEN-EN 1992-1-1:2005 [2] can be determined as follows:

$$V_{Rd,c} = C_{Rd,c} k \left(100 \rho_l f_{ck}\right)^{1/3} b_w d_l \geq v_{min} b_w d_l \tag{1}$$

$$k = 1 + \sqrt{\frac{200}{d_l}} \leq 2.0 \tag{2}$$

with:

$V_{Rd,c}$ the design shear capacity in [kN];

k the size effect factor, with d_l in [mm];

ρ_l the flexural reinforcement ratio;

f_{ck} the characteristic cylinder compressive strength of the concrete in [MPa];

b_w the web width of the section in [m];

d_l the effective depth to the main flexural reinforcement in [mm].

According to the Eurocode procedures, the values of $C_{Rd,c}$ and v_{min} may be chosen nationally. The default values are $C_{Rd,c}$ = $0.18/\gamma_c$ with γ_c=1.5 in general and v_{min} (f_{ck} in [MPa]):

$$v_{min} = 0.035 k^{3/2} f_{ck}^{1/2} \text{ in [MPa]} \tag{3}$$

NEN-EN 1992-1-1:2005 §6.2.2 (6) accounts for the influence of the shear span to depth ratio on direct load transfer. The contribution of a load applied within a distance $0.5d_l \leq a_v \leq 2d_l$ from the edge of a support to the shear force V_{Ed} may be multiplied by the reduction factor $\beta = a_v/2d_l$. In that clause of the code, the distance a_v is considered as the distance between the face of the load and the face of the support, or the center of the support for flexible supports.

The shear capacity according to the previously used Dutch code NEN 6720:1995 [3] can be verified with the following criterion:

$$\tau_d \leq \tau_1 \tag{4}$$

with τ_1 the ultimate flexural shear capacity of the concrete element without stirrups:

$$\tau_1 = 0.4 f_b k_\lambda k_h \sqrt[3]{w_o} \geq 0.4 f_b \tag{5}$$

with

f_b the concrete tensile strength, taken as the long-term tensile strength [4]:

$$f_{bm} = 0.7\left(1.05 + 0.05 f_{cm}\right) \tag{6}$$

k_λ for corbels and members at end supports where a compression strut can be formed between the load and the support; $k_\lambda = 1$ for all cases, except:

$$k_\lambda = \frac{12}{g_\lambda}\sqrt[3]{\frac{A_o}{b \times d_l}} \geq 1 \text{ with } \begin{array}{l} g_\lambda = 1 + \lambda_v^2 \text{ if } \lambda_v \geq 0.6 \\ g_\lambda = 2.5 - 3\lambda_v \text{ if } \lambda_v < 0.6 \end{array} \text{ and } \lambda_v = \frac{M_{dmax}}{dV_{dmax}} \tag{7}$$

λ_v the shear slenderness;

M_{dmax} the maximum absolute value of the design bending moment in the member

V_{dmax} the maximum absolute value of the design sectional shear in the member;

A_o is the smallest value of the area of the load or support, not exceeding $b \times d_l$;

k_h the size effect factor:

$$k_h = 1.6 - h \geq 1.0 \text{ with } h \text{ in [m]} \tag{8}$$

w_o the reinforcement percentage, for members without prestressing:

$$w_o = \frac{100 A_s}{b \times d_l} \leq 2.0 \text{ and } \geq 0.7 - 0.5\lambda_v \tag{9}$$

τ_d the shear stress in the section, $\tau_d = \frac{V_{Ed}}{b \times d_l}$.

As a result of these code changes, upon assessment a large number of existing Dutch reinforced concrete solid slab bridges are found to be insufficient for shear [5].

1.2. Assessment by Levels of Approximation

In the *fib* Model Code 2010 [6], the concept Levels of Approximation is introduced. Increasing the Level of Approximation increases the computational time, but also results in a closer estimation of the capacity. Levels of Approximation are used for the Model Code shear and punching provisions [6].

Levels of Approximation are also used in The Netherlands for the assessment of existing concrete structures, and in particular for the shear assessment of slab bridges [7]. These levels are called Levels of Assessment. The first Level of Assessment is the “Quick Scan” [8], a conservative spreadsheet-based method that results in a “Unity Check”: the ratio of the sectional shear stress caused by the dead load, superimposed loads and live loads to the shear capacity. If the Unity Check is larger than 1, the conclusion is not immediately that the bridge does not have sufficient capacity, but that the analysis has to be repeated at Level of Assessment II. At this Level, the shear stress distribution over the width of the support is determined with a linear elastic finite element program. The peak shear stress is then averaged over $4d_l$ (where d_l is the effective depth to the longitudinal reinforcement) [9] and compared to the shear capacity (same value as with Level of Assessment I) for the Level of Assessment II Unity Check. If the Unity Check is again larger than 1, the procedure is repeated at Level of Assessment III, which uses probabilistic analyses. Level of Assessment IV contains advanced non-linear finite element calculations and proof loading. As more advanced Levels of Assessment request more time and labor, it is preferred that the lower Levels of Assessment, namely Levels I and II, are able to reach sufficient accuracy.

1.3. Past research on shear in slabs

Over the past few years, research has been carried out at Delft University of Technology to study the behavior of reinforced concrete slab bridges. Experiments were carried out on slab specimens under concentrated loads close to supports [10-12]. It was concluded that slabs subjected to concentrated loads have additional shear capacity as a result of transverse load redistribution [13] when compared to beams. These conclusions were also supported by experimental evidence from the literature [14-20]. Theoretical studies led to the development of Yang's Critical Shear Displacement theory [21, 22]. For the shear analysis of slabs, the Extended Strip Model [23-25] was developed. Other suitable methods for advanced shear analysis of slabs, at Levels of Approximation III and IV, include the use of probabilistic analyses, non-linear finite element analyses [26] or using the Critical Shear Crack Theory [27], taking into account the non-axis-symmetric nature of the problem [28, 29] when slab bridges are analyzed.

The additional capacity of slabs has been taken into account in Level of Approximation I by the definition of an effective width in shear [7] at the slab support. In Level of Assessment II this approach resulted in the recommendation to distribute the peak stress over $4d_l$ [9, 30].

This paper looks at the highest Level of Assessment, which is field testing, and aims at estimating the conservativeness of the Level of Assessment I. In an exceptional case, an existing bridge, the Ruytenschildt Bridge in Friesland, was load tested to failure. Afterwards, beam specimens were sawn from the bridge and tested in the laboratory to further study the shear and flexural capacity of existing bridges. The field and laboratory testing of the same structure allow for a direct comparison between the different types of tests, Usually, this comparison is not possible because laboratory tests tend to be simplifications and schematizations of the reality. These tests are important, because field testing to failure of bridges is uncommon, and because the link between field and laboratory tests is not typically made,

1.4. Past load testing to failure

In the past, only a limited number of bridges have been tested to failure. An overview of those known by the authors is given in Table 1. It can be noted that the majority of these bridges were slab bridges, mostly resulting in a flexural failure. The testing of the Thurloxton underpass is not included [31], because the test was carried out after applying saw cuts over 1 m, so that only beam behavior and not slab behavior could be studied.

2. Description of Ruytenschildt Bridge

2.1. Introduction

The Ruytenschildt Bridge is located in the province of Friesland (the Netherlands), over a waterway connecting the Tjeuker Lake to the Vierhuister Course and in the national road N924 connecting the villages of Lemmer and Heerenveen. The bridge was built in 1962, and was scheduled for demolition and replacement by a bridge with a larger clearance for ship traffic, allowing for the passage of taller boats. The carriageway was divided into two lanes and a bike lane.

2.2. Geometry

The structure was a solid slab bridge with five spans. At the mid supports, cross-beams cast integrally onto the piers were used, and at the end supports the deck is cast into the abutments; the bridge is a fully integral bridge. The bridge had a skew angle of 18^o. The geometry is shown in Figure 1. The availability of at least one motor lane and one bicycle lane was needed during demolition and reconstruction. Therefore, the demolition of the bridge was planned in stages. In the first stage, 7.365 m of the bridge was demolished and the remaining 4.63 m served as one traffic lane. A saw cut between both parts was made, and the eastern part of the bridge of 7.365 m wide was tested to failure in spans 1 and 2. A separate temporary bike bridge on pontoons was provided. The slab thickness was about 550 mm.

2.3. Material Properties

62 cores were drilled to test the concrete compressive strength, showing that the average cube compressive strength was f_{cm} = 40 MPa [32]. Additional 31 concrete cores were drilled (in vertical and horizontal direction) from the beam specimens in the lab [33]. These additional tests provide a calibration factor for the poor surface treatment of the previously tested cores, resulting in f_{cm} = 63 MPa, which corresponds to a cylinder compressive strength $f_{cm,cyl}$ = 52 MPa. On the cores, the thickness of the asphalt layer was measured as 50 mm.

Reinforcement steel QR24 was used with diameters φ = 22 mm and φ = 19 mm for the longitudinal reinforcement and with diameter φ = 12 mm for the transverse reinforcement. QR24 steel has a characteristic yield strength f_{yk} = 240 MPa. The reinforcement layout is shown in Figure 2. Tensile tests on steel samples taken from the structure showed an average yield strength f_y = 352 MPa and an average tensile strength f_t = 435 MPa for the bars with a diameter φ of 12 mm and f_y = 309 MPa and f_t = 360 MPa for φ = 22 mm. The samples were taken from the bridge after testing, so that yielding of the steel could have occurred before determining the material properties. This suspicion seems to be confirmed by the limited yielding plateau that was obtained in the measured load-deformation relationship of the steel samples. Past testing of QR24 steel from a similar bridge gave f_y = 282 MPa and f_t = 402 MPa [34].

2.4. State of Ruytenschildt bridge prior to testing

In 2004 [35], a thorough inspection of the bridge was carried out. The following structural problems were identified: cracking in the concrete slab over the entire depth of the cross-section (identified by the presence of water drops on the soffit of the slab), local signs of rebar corrosion, clogging of the drainage pipes, and degradation of the timber sheet piles used at the abutment. The depth of carbonation was identified as 1 – 2 mm, which is well within the concrete cover, and the chloride content was measured on four samples, of which two had large amounts of chloride. Other sources of material degradation were not measured.

A few weeks prior to the testing of the bridge, a visual inspection was carried out. This inspection identified again clogging of the drainage pipes, longitudinal and transverse cracks on the bottom and side faces of the slab, and a few locations with concrete damage caused by rebar corrosion.

3. Results of field testing of the Ruytenschildt bridge

3.1. Test setup at bridge site

The geometry of the tandem load of NEN-EN 1991-2:2003 [36] was used for the test, with wheel prints of 400 mm × 400 mm , a distance along the width between the wheels of 2 m and an axle distance of 1.2 m. The face-to-face distance between axle and cross-beam was $2.5d_l$ (1250 mm), which is the critical position for shear failure [5, 37]. The distance between the saw cut line and the first wheel was 800 mm in span 1 and 600 mm in span 2. The tandem was placed in the obtuse angle, since this location is critical for shear [38].

For a safe execution of the experiment, a steel load spreader, see Figure 3, was applied over the span. Before the experiment, ballast blocks were placed on the load spreader, but the jacks were not yet extended, so that the slab was not loaded. During the experiment, the hydraulic jacks were gradually extended, and so the load was gradually transferred from the load spreader to the wheel prints positioned on top of the concrete slab. If large deformations caused by failure would occur, the load on the jacks would decrease again thanks to this structure.

During the proof loading and testing to failure of the Ruytenschildt bridge, the structure was instrumented to study the vertical and horizontal deformations, crack width, and to register cracking activities with acoustic emission measurements. The vertical deformations were measured with linear variable differential transformers (LVDTs) and laser triangulation sensors. The deformations on the bottom surface, indicating the average strain over 1 m, were measured by LVDTs. The opening of existing cracks was followed with LVDTs. An interpretation of the measurements gathered during the field test and their indication of the structure deviating from linear behaviour is outside of the scope of this paper, which studies the ultimate limit state.

3.2. Measurements on Ruytenschildt Bridge

Two tests were carried out on the bridge: one test in span 1 and a second test in span 2, two days later. Several load cycles were applied during the field test, but only the last cycles of loading until the ultimate capacity are discussed here.

For span 2, the measurement scheme and the position of the tandem are given in Figure 4. The reference for the LVDTs and lasers was drop wire. The loading scheme for the final step for span 1 is given in Figure 5a, and for span 2 in Figure 5b. The load-displacement diagram of testing in span 2 as measured at one of the laser triangulation sensors is given in Figure 6.

The maximum load during the test on span 1 was 3049 kN, but failure was not achieved as the maximum load was determined by the maximum available counter weight. Flexural cracking was observed in span 1, and no damage occurred at support 2. The test in span 1 did not cause additional precracking on span 2. For testing on span 2, two days later, additional counter weight was ordered. The maximum load was 3991 kN. Flexural failure was achieved. A settlement at the pier of 15 mm right after achieving the maximum load was observed. After removing all loading and measurement equipment, delayed recovery resulted in a final residual settlement of 8 mm.

3.3. Calculated and tested capacity

3.3.1. Shear capacity of Ruytenschildt Bridge

To predict the capacity of the tested cross-sections, calculations were performed with average material parameters as given in §2.3. The characteristic shear capacity from NEN-EN 1992-1-1:2005 §6.2.2. [2], see Eq. (1), can be converted into an average shear capacity by using f_{cm} and $C_{Rm,c}$ = 0.15 [39]:

$$v_{R,c} = C_{Rm,c} k (100 \rho_l f_{cm})^{1/3} \tag{10}$$

For skewed slabs, the determination of the effective width in shear is ambiguous and a direct application of the recommendations for straight slabs is not possible. Three options have been studied: b_{str}, the effective width for a straight slab, b_{skew} with horizontal load spreading under 45^o from the far side of the wheel print to the face of the support [7], and b_{para} based on a parallel load spreading to the straight case, as shown in Figure 7.

The maximum total tandem load resulting in a Unity Check of 1 was estimated: the maximum load is sought so that the resulting shear stress at the support from all occurring loads equals the shear capacity from Eq. (1). The recommendations from the slab shear experiments are taken into account [5]. However, knowledge on how the plain bars affect the shear capacity is not available. Therefore, the same expressions as for deformed bars are used to estimate the shear capacity. Previous research on beams with plain bars [40-43] showed a higher shear capacity than for beams with deformed bars. It can thus be thought that the provided values are a lower bound of the real shear capacity of the bridge.

The maximum calculated tandem load is given as P_{tot} in Table 2. From the slab shear experiments [10], the 5% lower bound of the ratio of the tested to predicted (Eq. 1) shear capacity was found to be 1.466 [44], mainly caused by transverse load redistribution. Multiplying P_{tot} by 1.466 gives $P_{tot,slab}$ in Table 2. This multiplication factor was derived in experiments on straight slabs. Skewed slabs, on the other hand, have larger stress concentrations in the obtuse corner, which could lead to smaller capacities [45]. Therefore, the full increase of the maximum load with the factor 1.466 cannot immediately be extrapolated to skewed slabs, so that the shear capacity is estimated in between P_{tot} and $P_{tot,slab}$. The sixth row of Table 2 shows the maximum load in the experiment.

For span 1, the maximum experimental load was smaller than the predicted maximum P_{tot}. If the slab effect is considered, then the maximum calculated load $P_{tot,slab}$ is significantly higher than the experimental load. For span 2, similar conclusions can be drawn. Since the slab failed in flexure, there is no indication of its ultimate shear capacity.

Finally, it needs to be remarked that the influence of the integrally cast cross-beam was not accounted for in the calculations. The cross-beams induce some restraint that counteracts the shear. The longitudinal confinement caused by the support moments possibly causes an increase in the shear capacity. A quantification of this effect is outside of the scope of this study.

3.3.2. Bending moment capacity of Ruytenschildt Bridge

To determine the moment at cracking M_{cr}, yielding M_y, and the ultimate M_u, traditional beam analyses are carried out, see Table 2. The calculations are based on average material properties. The cracking moment is based on the flexural tensile strength of the concrete, calculated based on the ACI 318-14 [46] expression (function of the concrete compressive strength). For the moment at yielding, the stress-strain diagram of the concrete is approximated with Thorenfeldt’s parabola. The ultimate moment M_u is conservatively based on f_t = 360 MPa and is determined using Whitney’s stress block for the concrete under compression. To find the maximum experimental moment, M_{test}, the two axles of the proof load tandem are applied as two point loads on a beam model of five spans, and the self-weight is applied as a distributed load.

The Ruytenschildt Bridge is an integral bridge, and a moment will develop at support 1. Because the rotational stiffness of support 1 is difficult to estimate, it was conservatively estimated as a hinge. In reality, a support moment develops which decreases the span moment, explaining why failure did not occur at M_{test} for testing in span 1.

For span 2, M_{test} lies in between M_y and M_u, which corresponds with the experiment: span 2 failed in flexure in the span; yielding of the steel was observed but crushing of the concrete was not achieved.

The Ruytenschildt Bridge had identical span lengths for all five spans. Most continuous bridges have shorter end spans, which would result in different values for shear and moment.

4. Description of beams sawn from the Ruytenschildt Bridge

4.1. Introduction

Before the remaining part of the bridge was demolished, beams were extracted from the spans that were not tested in the field so they could be tested in the laboratory. On these beams, the transverse redistribution that occurs in slabs can be excluded. The effects of the skew angle are excluded as well. Thus, the measured shear or flexural behavior can be directly compared with the code provisions for beams, which are the basis of the calculations presented previously.

Two topics that were of interest for further studies and that were analyzed in the beam tests are the effect of plain reinforcement bars on the shear capacity, the occurring failure mode (is shear failure even realistic?), and the additional deformation capacity after the yielding moment of a critical section is reached. Studying these aspects may lead to an improved understanding and assessment of existing bridges.

4.2. Geometry of the sawn beams

Three beams, RSB01-RSB03, of 6 m were sawn from span 1. The positions of the beams in the deck are indicated in Figure 2. The intended width of the specimens was 500 mm for RSB01 and RSB02, and 1000 mm for RSB03. The sawing operation at the site of the viaduct was not a precise process. As a result, the width of the beams was larger than originally intended. Therefore, the actual cross-sections of the specimens were measured at five positions: at 0.6 m, 1.8 m, 3.0 m, 4.2 m and 5.4 m from the end of the specimens, resulting in an overview of the cross-sections as given in Figure 8a.

The asphalt layer was kept on the specimens. The average thickness of the layer is 50 mm. This layer was only removed at the loading plate (except for RSB03A) and the top surface was leveled with high strength mortar. This treatment ensures that the poor mechanical properties of the asphalt will not influence the loading process. On the remaining parts of the beam, the asphalt layer was kept to maintain the flexural stiffness of the original bridge and the original dead load state that included the superimposed dead load. In order to check the influence of removing the asphalt layer, in test RSB03A the asphalt layer is kept.

According to Figure 2, the longitudinal reinforcement configuration is repeated at every 270 mm. It is grouped into 4 layers; the details of each layer are shown in Figure 8b. The bars are arranged in the direction of the shorter edge of the deck. The saw cut lines of the beams were in the transverse direction, see Figure 2. Thus, the longitudinal bars were not aligned with the saw cut. The positions of the bars with respect to the saw cut in the longitudinal direction are not consistent among the beams, therefore these positions have to be checked individually. The actual positions of the saw cuts in comparison with the longitudinal reinforcement layout are indicated in Figure 8b and Figure 9, determining the positions of the support. Take RSB01 for example: the supports were placed closer to end B, because the Ø19 rebar in layer 4 is closer to the B end.

Similarly, the availability of the reinforcement is checked in the width direction. For all three specimens, the sawing operation affects the longitudinal bars at the edges, see Figure 8a and b. These partial bars are not taken into account for the shear capacity. For the flexural capacity of sections more than 1 m away from the damaged rebar, these bars are accounted for. The calculated anchorage length according to NEN-EN 1992-1-1:2005 Eq. 8.3 [2] is 452 mm. The applied anchorage length (1 m) is more than double the code requirement to compensate for the potentially weaker bond between plain rebar and concrete. Similar considerations determine the positions of the supports. Based on the reinforcement configuration sketched in Figure 8b, the sectional and reinforcement properties are given in Figure 9 and Table 3.

4.3. Test setup

The specimens are simply supported with a span of 5 m and loaded by a point load. The position of the point load varies according to the type of test. For the bending tests (RSB01F and RSB03F, with “F” for flexural test), the point load is located at midspan. For the shear test, the loading position is at 1.25 m from the support in RSB02A and RSB02B and at 1.3 m in RSB03A, with “A” or “B” denoting the support close to which was tested. The loading geometry of all tests is indicated in Figure 9. During the experiments, the magnitude of the load, vertical deflections and crack widths were measured. In all tests, the deflection at the loading point was measured from the bottom of the specimen (on both sides of the beam). The support deformation was compensated from the measurements. A typical load-deflection relationship of specimens failing in flexure and in shear are given in Figure 10a and 10b respectively. Acoustic emission measurements were used to study crack development and propagation.

In total 5 tests were executed on 3 specimens, among which, two tests were carried out on specimens RSB02 and RSB03. On RSB02, the first test was RSB02A. By the end of that test, a flexural shear crack was formed, nevertheless, the specimen did not collapse after the formation of the crack. Instead, a yielding plateau was observed in the load-deflection relationship. In order to guarantee the structural integrity for the test RSB02B, the test was stopped with limited deflection. The loading point was moved to the B end, where a flexural shear failure was found. In the case of RSB03, similar approach was taken. The first test of the specimen was a flexural test RSB03F. Afterwards, the shear test was executed. During the whole experimental program, the position of the supports was not changed. According to [21], it is assumed that this will not affect the crack pattern of the specimen, and eventually the shear capacity. This is further validated in the experiments reported in [39, 47].

5. Test results of beams

5.1. Overview of results

The theoretical yield moment M_y, the shear capacity according to the Eurocode provisions (Eq. 1) $V_{u,EC}$, and according to Yang's Critical Shear Displacement theory (CSD), $V_{u,CSD}$ [21, 22] are listed in Table 4. The calculated values are determined by using the average cross-sectional properties from Figure 8a. The experimental sectional shear V_u and maximum load P_u are also given in Table 4. The critical shear crack is assumed at 1 m from the closest support. P_y is the calculated load at yielding in the critical cross-section. $P_{s,EC}$ is the calculated load for shear failure according to NEN-EN 1992-1-1:2005 §6.2.2., see Eq. (1). $P_{s,CSD}$ is the calculated load for shear failure according to the Critical Shear Displacement theory proposed in [21, 22]. $P_{cal,1}$ is the minimum of P_y and $P_{s,EC}$ and $P_{cal,2}$ of P_y and $P_{s,CSD}$.

5.2. Shear Behavior

In both RSB02A and RSB02B, an inclined crack developed in the shear span. The formation of this crack did not result in a drop of the capacity of the specimen. In RSB02B, an inclined crack was observed before yielding of the longitudinal reinforcement. The test was stopped by then to ensure the structural integrity for the test RSB02A. After that, a second test at end B was done as the continuation of RSB02B. The same loading position did not result in a significant additional deflection. Failure then occurred by crushing of the compression strut. In RSB03A, the shear span was increased to 1.3 m, resulting in failure by forming an inclined crack in the shear span.

In the literature [42, 48], larger shear capacities are found for beams reinforced with plain bars than for beams with deformed bars. However, when studying the shear tests presented here, the experimental shear capacities are not significantly different from the calculated shear capacities based on models for specimens with deformed bars. Similar conclusions were drawn in the past from tests on slabs reinforced with plain bars as compared to deformed bars, subjected to concentrated loads close to supports [49]. The expression given by Eurocode Eq (1), turns out to give a reasonable estimation of the test results, with an average ratio of tested to predicted values of 1.2 and a coefficient of variation of 5.2%. This difference partially contributes to the underestimation of the ultimate capacity of the bridge during the test preparation phase.

A comparison with Yang's Critical Shear Displacement Theory shows an average ratio of tested to predicted results of 0.95 and a coefficient of variation of 4.8%.

When linking the results of the beam tests to the capacity of the bridge tested in the field, it must be noted that the longitudinal confinement, effects of continuity, and the transverse redistribution capacity of the slab will increase the shear capacity beyond the capacity as quantified on the beam. The results of the beam test and the field test can be linked, as similar shear spans were used in these tests. These effects also result in a shift of the failure mode for existing slab bridges: flexural failures become more probable and shear failures less probable.

5.3. Flexural Behavior

The comparison between experimental and calculated values shows that the prediction of the yielding moment is accurate, with a difference of maximum 2%. Additionally, it was confirmed that beams with plain bars have large rotational capacities. In RSB01F, the residual deformation was more than 125 mm (250 mm/2, see Figure 11c and d), which is 1/40 of the span length. The test had to be stopped because the maximum displacement of the actuator was reached. The load level before the stop of the test was still 271 kN, while the peak load was 274 kN.

6. Recommendations

From the field testing, the following recommendations can be given:

- Further research is necessary to identify the effect of the skew angle on the shear capacity. Meanwhile, the uncertainties can be covered by applying the different effective widths from Figure 7, and to define a range of values between which shear failure could occur.
- An initial shear assessment can be carried out with the Quick Scan method [8].

From the laboratory testing, the following recommendations can be given:

- The shear capacity can be predicted with the shear provisions from Eurocode 2 [2], as well as with Yang’s Critical Shear Displacement Theory [21, 22].
- In structures with plain reinforcement bars with a low yield strength, shear failures can occur, which was contrary to the expectation. Therefore, further experimental work on the flexural and shear capacity of beams with low levels of reinforcement is under development.
- The shear capacity of elements with plain reinforcement bars can be determined in the same way as the shear capacity of elements with ribbed bars.

7. Summary and Conclusions

This paper presented a test to failure executed in the field on a reinforced concrete slab bridge from 1962, as well as on three beams sawn from the bridge. A literature review showed that collapse tests on reinforced concrete slab bridges are scarce. This observation motivated the authors to carry out a well-instrumented collapse test on an existing bridge, and extend this research with the testing of beams in the laboratory.

Two spans were tested in the field. In the first span, flexural distress was observed, but failure did not occur. One of the reasons why the flexural capacity was higher in span 1 than predicted, is that the tested bridge was an integral bridge. The effect of the support moment resulted in a higher moment capacity in the span than when assuming hinges. In the second span, more counterweight was provided and a flexural failure could be achieved. Despite the effect of the different boundary conditions, the flexural capacity of the tested bridge could be estimated satisfactorily. However, the test showed that the shear capacity of the bridge deck was higher.

The beams tested in the lab failed in shear and flexure. As such, shear failures cannot be excluded for elements with plain reinforcement. Moreover, a larger shear capacity for beams reinforced with plain bars than with deformed bars was not observed in the lab experiments.

A final conclusion of the presented research is that the current rating procedures at Level of Assessment I (the Quick Scan method) are conservative for existing reinforced concrete slab bridges.

Acknowledgements

The authors wish to express their gratitude and sincere appreciation to the Province of Friesland and the Dutch Ministry of Infrastructure and the Environment (Rijkswaterstaat) for financing this research work. The contributions and help of our colleagues A. Bosman, S. Fennis and P. van Hemert, of the contractor de Boer en de Groot and of Mammoet, responsible for applying the load, are also gratefully acknowledged.

List of notations

a_v face-to-face distance between load and support

b member width

b_{edge} distance between free edge and load

b_{para} effective width based on a parallel load spreading to the straight case

b_{skew} effective width with horizontal load spreading under 45^o from the far side of the wheel print to the face of the support

b_{str} effective width for a straight slab

b_w web width

d_l effective depth to the longitudinal reinforcement

f_b the long-term concrete tensile strnegth

f_{ck} characteristic compressive strength (lower 5% bound)

f_{cm} average cube compressive strength

$f_{cm,cyl}$ average cylinder compressive strength

f_t average tensile strength of reinforcement steel

f_y average yield strength of reinforcement steel

f_{yk} characteristic yield strength of steel

g_λ a parameter depending on the shear slenderness

h member thickness

k size effect factor

k_h size effect factor from the Dutch NEN 6720:1995

k_λ a factor to take continuity at the support into account

q_w distributed load representing the self-weight

v_{min} lower bound of the shear capacity

$v_{R,c}$ average shear capacity

w_o reinforcement percentage, which needs to fulfill maximum and minimum values

A_c area of the concrete cross-section

A_o area used in NEN 6720:1995

A_s area of steel

$C_{Rd,c}$ calibration factor in shear formula to determine the design shear capacity

$C_{Rm,c}$ calibration factor in shear formula to determine the average shear capacity

M_{cr} calculated moment at cracking of the cross-section

M_{dmax} maximum absolute value of the design bending moment in the member

M_{test} maximum moment on the cross-section during the experiment

M_u calculated moment at the ultimate of the cross-section

M_y calculated moment at yielding of the cross-section

$P_{cal,1}$ minimum of P_y and $P_{s,EC}$

$P_{cal,2}$ minimum of P_y and $P_{s,CSD}$.

$P_{s,CSD}$ calculated load for shear failure according to the Critical Shear Displacement theory

$P_{s,EC}$ calculated load for shear failure according to NEN-EN 1992-1-1:2005 §6.2.2

P_{tot} calculated maximum load at shear failure on tandem

$P_{tot,slab}$ calculated maximum load at shear failure on tandem after multiplying with slab increase factor

P_u maximum load during experiment

P_y calculated load at yielding in the critical cross-section

V_{dmax} maximum absolute value of the sectional shear in the member

V_{Ed} design sectional shear force for the considered ULS load combination

$V_{Rd,c}$ design shear capacity according to the Eurocode provisions

V_u experimental sectional shear

$V_{u,CSD}$ shear capacity according to Yang’s Critical Shear Displacement theory (CSD)

$V_{u,EC}$ mean shear capacity according to the Eurocode provisions

γ_c partial factor for concrete material

φ reinforcement bar diameter

λ_v shear slenderness

ρ_l reinforcement ratio of the longitudinal tensile reinforcement

τ_d design shear stress for the considered ULS load combination

τ_1 concrete contribution to the shear capacity

References

[1] Code Committee 351001. Eurocode 1 - Actions on structures - Part 2: Traffic loads on bridges, NEN-EN 1991-2/NA:2011. Delft, The Netherlands: Civil engineering center for research and regulation, Dutch Normalization Institute; 2011. p. 38.

[2] CEN. Eurocode 2: Design of Concrete Structures - Part 1-1 General Rules and Rules for Buildings. NEN-EN 1992-1-1:2005. Brussels, Belgium: Comité Européen de Normalisation; 2005. p. 229.

[3] Code Committee 351001. NEN 6720 Technical Guidelines for Strucutres, Provisions Concrete TGB 1990 – Structural Requirements and Calculations Methods (VBC 1995). Delft, The Netherlands: Civieltechnisch centrum uitvoering research en regelgeving, Nederlands Normalisatie-instituut, 1995. (in Dutch)

[4] CUR. CUR Report 94-13, 1994, Background to VBC 1990. Gouda, The Netherlands: Civieltechnisch Centrum Uitvoering Research en Regelgeving; 1994. p. 162. (in Dutch)

[5] Lantsoght EOL, van der Veen C, de Boer A, Walraven JC. Recommendations for the Shear Assessment of Reinforced Concrete Slab Bridges from Experiments Structural Engineering International. 2013;23:418-26.

[6] fib. Model code 2010: final draft. Lausanne: International Federation for Structural Concrete; 2012.

[7] Lantsoght EOL, de Boer A, van der Veen C, Walraven J. Effective shear width of concrete slab bridges. Proceedings of the Institution of Civil Engineers – Bridge Engineering. 2015;168:287-98.

[8] Vergoossen R, Naaktgeboren M, ‘t Hart M, De Boer A, Van Vugt E. Quick Scan on Shear in Existing Slab Type Viaducts. International IABSE Conference, Assessment, Upgrading and Refurbishment of Infrastructures. Rotterdam, The Netherlands, 2013. p. 8.

[9] Lantsoght EOL, De Boer A, van der Veen C. Determination of distribution width for shear stresses at support in reinforced concrete slab bridges. EuroC. St. Anton am Arlberg, Austria2014. p. 9

[10] Lantsoght EOL, van der Veen C, Walraven JC. Shear in One-way Slabs under a Concentrated Load close to the support. ACI Structural Journal. 2013;110:275-84.

[11] Lantsoght EOL, van der Veen C, De Boer A, Walraven J. Influence of Width on Shear Capacity of Reinforced Concrete Members. ACI Structural Journal. 2014;111:1441-50.

[12] Lantsoght EOL, van der Veen C, Walraven J, de Boer A. Experimental investigation on shear capacity of reinforced concrete slabs with plain bars and slabs on elastomeric bearings. Engineering Structures. 2015;103:1-14.

[13] Lantsoght EOL, van der Veen C, de Boer A, Walraven J. Transverse Load Redistribution and Effective Shear Width in Reinforced Concrete Slabs. Heron. in press:29 pp. .

[14] Graf O. Experiments on the Capacity of Reinforced Concrete Slabs under a concentrated Load close to a Support. Deutscher Ausschuss für Eisenbeton. 1933;73:10-6. (in German)

[15] Regan PE. Shear Resistance of Concrete Slabs at Concentrated Loads close to Supports. London, United Kingdom: Polytechnic of Central London; 1982. p. 24.

[16] Furuuchi H, Takahashi Y, Ueda T, Kakuta Y. Effective width for shear failure of RC deep slabs. Transactions of the Japan concrete institute. 1998;20:209-16.
[17] Reißen K, Hegger J. Experimental investigations on the effective width for shear of single span bridge deck slabs. Beton- und Stahlbetonbau. 2013;108:96-103. (in German)
[18] Reißen K, Hegger J. Experimental Investigationson the shear capacity of RC cantilever bridge deck slabs under concentrated loads - influences of moment-shear ratio and an inclined compression zone. European Bridge Conference. Edinburgh, UK, 2015. p. 13.
[19] Rombach GA, Latte S. Shear resistance of bridge decks without shear reinforcement. International FIB Symposium 2008. Amsterdam, The Netherlands: Fédération Internationale du Béton; 2008. p. 519-25.
[20] Natário F, Ruiz MF, Muttoni A. Shear strength of RC slabs under concentrated loads near clamped linear supports. Engineering Structures. 2014;76:10-23.
[21] Yang Y. Shear Behaviour of Reinforced Concrete Members without Shear Reinforcement - A New Look at an Old Problem. Ph.D. Thesis Delft: Delft University of Technology; 2014.
[22] Yang Y, Den Uijl JA, Walraven J. The Critical Shear Displacement theory: on the way to extending the scope of shear design and assessment for members without shear reinforcement. Structural Concrete. 2016 (available online ahead of print): 25 pp.
[23] Lantsoght EOL, van der Veen C, de Boer A. Predicting the Shear Capacity of Reinforced Concrete Slabs subjected to Concentrated Loads close to Supports with the Modified Bond Model. IABSE 2014, Engineering for Progress, Nature and People. Madrid, Spain2014.
[24] Lantsoght EOL, van der Veen C, de Boer A. Modified Bond Model for Shear in Slabs under Concentrated Loads. In: Stang H, Braestrup M, editors. fib Symposium Copenhagen: Concrete Innovation and Design. Kopenhagen, 2015. p. 10.
[25] Lantsoght EOL, Van der Veen C, De Boer A, Alexander SDB. Bridging the gap between one-way and two-way shear in slabs. ACI Special Publication for the International Punching Symposium. 2016 (in review):20.
[26] Belletti B, Damoni C, Hendriks MAN, de Boer A. Analytical and numerical evaluation of the design shear resistance of reinforced concrete slabs. Structural Concrete. 2014;15:317-30.
[27] Muttoni A, Fernández Ruiz M. Shear strength in one- and two-way slabs according to the Critical Shear Crack Theory. International FIB Symposium 2008. Amsterdam, The Netherlands: Fédération Internationale du Béton 2008. p. 559-63.
[28] Sagaseta J, Muttoni A, Ruiz MF, Tassinari L. Non-axis-symmetrical punching shear around internal columns of RC slabs without transverse reinforcement. Magazine of Concrete Research. 2011;63:441-57.
[29] Falbr J. Shear redistribution in solid concrete slabs. M.Sc. Thesis, Delft: Delft University of Technology; 2011.
[30] Lantsoght EOL, de Boer A, Van der Veen C, Walraven JC. Peak shear stress distribution in finite element models of concrete slabs. In: Zingoni A, editor. Research and Applications in Structural Engineering, Mechanics and Computation. Cape Town, South Africa: Taylor and Francis; 2013. p. 475-80.
[31] Cullington DW, Daly AF, Hill ME. Assessment of reinforced concrete bridges: Collapse tests on Thurloxton underpass. Bridge Management. 1996;3:667-74.
[32] Lantsoght EOL. Ruytenschildt Bridge: analysis of test results at the ultimate limit state. Stevin Report 25.5-15-05. Delft, The Netherlands: Delft University of Technology; 2015. p. 89. (in Dutch)

[33] Yang Y. Experimental Studies on the Structural Behaviours of Beams from Ruytenschildt Bridge. Stevin Report 25.5-15-09, 2015. p. 61.
[34] Yang Y, Den Uijl JA, Dieteren G, de Boer A. Shear capacity of 50 years old reinforced cocnrete bridge deck without shear reinforcement. 3rd fib International Congress. Washington DC, USA: fib; 2010. p. 12.
[35] de Pee J. Inspection report Ruytenschildt Bridge. Nebest, BV; 2004. (in Dutch)
[36] CEN. Eurocode 1: Actions on structures - Part 2: Traffic loads on bridges, NEN-EN 1991-2:2003. Brussels, Belgium: Comité Européen de Normalisation; 2003. p. 168.
[37] Rijkswaterstaat. Guidelines Assessment Bridges - Rating of structural safety of an existing bridge at repair, usage and disapproval. 2013. p. 117. (in Dutch)
[38] Cope RJ. Flexural Shear Failure of Reinforced-Concrete Slab Bridges. Proceedings of the Institution of Civil Engineers Part 2-Research and Theory. 1985;79:559-83.
[39] Yang Y, den Uijl JA. Report of Experimental Research on Shear Capacity of Beams Close to Intermediate Supports. Stevin Report 25.5-11-10. Delft: Delft University of Technology; 2011.
[40] Kani GNJ. The Riddle of Shear Failure and Its Solution. ACI Journal Proceedings. 1964;61:441-67.
[41] Muttoni A, Ruiz MF. Shear strength of members without transverse reinforcement as function of critical shear crack width. ACI Structural Journal. 2008;105:163-72.
[42] Leonhardt F, Walther R. The Stuttgart shear tests, 1961; contributions to the treatment of the problems of shear in reinforced concrete construction. London: Cement and Concrete Association; 1962.
[43] Iyengar KTSR, Rangan BV, Palaniswamy R. Some factors affecting the shear strength of reinforced concrete beams. Indian Concrete Journal. 1988;42:499-505.
[44] Lantsoght EOL. Progress Report: Experiments on slabs in reinforced concrete - Part II: Analysis of Results. Stevin Report 25.5-12-10. Delft University of Technology, The Netherlands; 2012. p. 289 pp.
[45] Cope RJ, Rao PV, Edwards KR. Shear in skew reinforced concrete slab bridges – analytical and experimental studies – A report to the Department of Transport. Liverpool, UK: University of Liverpool; 1983. p. 219.
[46] ACI Committee 318. Building code requirements for structural concrete (ACI 318-14) and commentary. Farmington Hills, MI: American Concrete Institute; 2014.
[47] Yang Y, den Uijl JA, Walraven J. Shear Capacity of Reinforced Concrete Beams under Complex Loading Conditions. the 9th fib International PhD Symposium in Civil Engineering. Karlsruhe: Karlsruhe Institude of Technology; 2012. p. 43-8.
[48] Kani MW, Huggins MW, Wittkopp RR. Kani on Shear in Reinforced Concrete. Canada, 1979.
[49] Lantsoght EOL. Shear in Reinforced Concrete Slabs under Concentrated Loads Close to Supports: Delft University of Technology; PhD Thesis; 2013.
[50] Haritos N, Hira A, Mendis P, Heywood R, Giufre A. Load testing to collapse limit state of Barr Creek Bridge. Transportation Research Record. 2000:A92-A102.
[51] Azizinamini A, Boothby TE, Shekar Y, Barnhill G. Old Concrete Slab Bridges. 1. Experimental Investigation. Journal of Structural Engineering-ASCE. 1994;120:3284-304.
[52] Azizinamini A, Shekar Y, Boothby TE, Barnhill G. Old concrete slab bridges. 2: Analysis. Journal of Structural Engineering-ASCE. 1994;120:3305-19.

[53] Miller RA, Aktan AE, Shahrooz BM. Destructive testing of decommisisioned concrete slab bridge. Journal of Structural Engineering-ASCE. 1994;120:2176-98.
[54] Aktan AE, Zwick M, Miller R, Shahrooz B. Nondestructive and Destructive Testing of Decommissioned Reinforced Concrete Slab Highway Bridge and Associated Analytical Studies. Transportation Research Record: Journal of the Transportation Research Board. 1992;1371:142-53.
[55] Jorgenson JL, Larson W. Field Testing of a Reinforced Concrete Highway Bridge to Collapse. Transportation Research Record: Journal of the Transportation Research Board. 1976;607:66-71.
[56] Bagge N, Shu J, Plos M, Elfgren L. Punching Capacity of a Reinforced Concrete Bridge Deck Slab Loaded to Failure. IABSE 20152015.
[57] Bagge N, Sas G, Nilimaa J, Blanksvard T, Elfgren L, Tu Y et al. Loading to failure of a 55 year old prestressed concrete bridge. IABSE Workshop. Helsinki, Finland, 2015. p. 130-7.

List of tables and figures

List of Tables:

List of Figures:

Figure 11 - Photographs of beams tests: (a, b) rebar damage of RSB03, end A; (c) crack caused by flexural failure of RSB01; (d, e) residual deformation of RSB01 after failure.

Table 1 – Overview of past testing to failure on bridges.

Reference	Bridge name	Type of bridge	Failure mode
Haritos et al., 2000 [50]	Barr Creek	slab bridge	Flexural failure
Azizinamini et al., 1994 [51, 52]	Niobrara River	slab bridge	Flexural failure
Miller et al., 1994 [53, 54]	-	slab bridge	Punching failure
Jorgenson & Larson, 1976 [55]	ND-18	slab bridge	Flexural failure
Bagge et al., 2015 [56, 57]	Kiruna	prestressed girder bridge	Punching failure

Table 2 - Calculated shear and moment capacity of tested spans.

Span	**Span 1**		**Span 2**	
Shear capacity	P_{tot} (kN)	$P_{tot,slab}$ (kN)	P_{tot} (kN)	$P_{tot,slab}$ (kN)
$\boldsymbol{b_{str}}$	3760	5512	4224	6192
$\boldsymbol{b_{para}}$	3236	4744	3608	5289
$\boldsymbol{b_{skew}}$	4804	7043	5596	8204
Experiment	3049		3991	
Flexural capacity	**Span moment**		**Support moment**	**Span moment**
$\boldsymbol{M_{cr}}$ **(kNm)**	1816		1690	1592
$\boldsymbol{M_{y}}$ **(kNm)**	3489		5174	3412
$\boldsymbol{M_{u}}$ **(kNm)**	4964		7064	4705

M_{test} (kNm)	4889	3306	4188

Table 3 - Properties of critical cross-sections of the beams.

	RSB01F	**RSB02A**	**RSB02B**	**RSB03F**	**RSB03A**
d_l (mm)	503.0	515.5	520.0	521	515
A_c (m^2)	0.290	0.297	0.3066	0.596	0.537
Rebar	4Ø22+4Ø19	4Ø22+4Ø19	4Ø22+5Ø19	9Ø22+8Ø19	7Ø22+8Ø19
ρ_l	0.91%	0.89%	0.96%	0.95%	0.92%

Table 4 - Comparison of test results and model predictions.

	M_y (kNm)	**$V_{u,EC}$ (kN)**	**$V_{u,CSD}$ (kN)**	**V_u (kN)**	**P_y (kN)**	**$P_{s,EC}$ (kN)**	**$P_{s,CSD}$ (kN)**	**P_u (kN)**	**$P_u/P_{cal,1}$**	**$P_u/P_{cal,2}$**
RSB01F	369.2	245.4	275.9	149.9	275.8	466.8	443.4	275.8*	1.00	1.00
RSB02A	378.3	254.4	327.5	289.1	376.2	322.5	420.0	368.7*	1.14	0.98
RSB02B	422.5	260.3	338.8	330.7†	423.4	331.2	435.4	415.8†	1.26	0.98
RSB03F	819.0	480.3	468.2	326.5	617.3	914.1	889.9	606.6*	0.98	0.98
RSB03A	809.3	469.9	603.1	546.2	792.0	603.7	783.7	706.7‡	1.17	0.90

† The load dropped due to the formation of an inclined crack. The test was stopped to keep the integrity of the specimen for another test at end A. Later, a second test was executed at the same load position. It turned out that the load level could be increased further to 424.2 kN when the compression zone of the specimen failed. Thus, V_u is determined for P_u = 424.2 kN.

‡ Flexural shear failure

* Flexural failure

Figure 1

Click here to download Figure: fig 1_yyg.eps

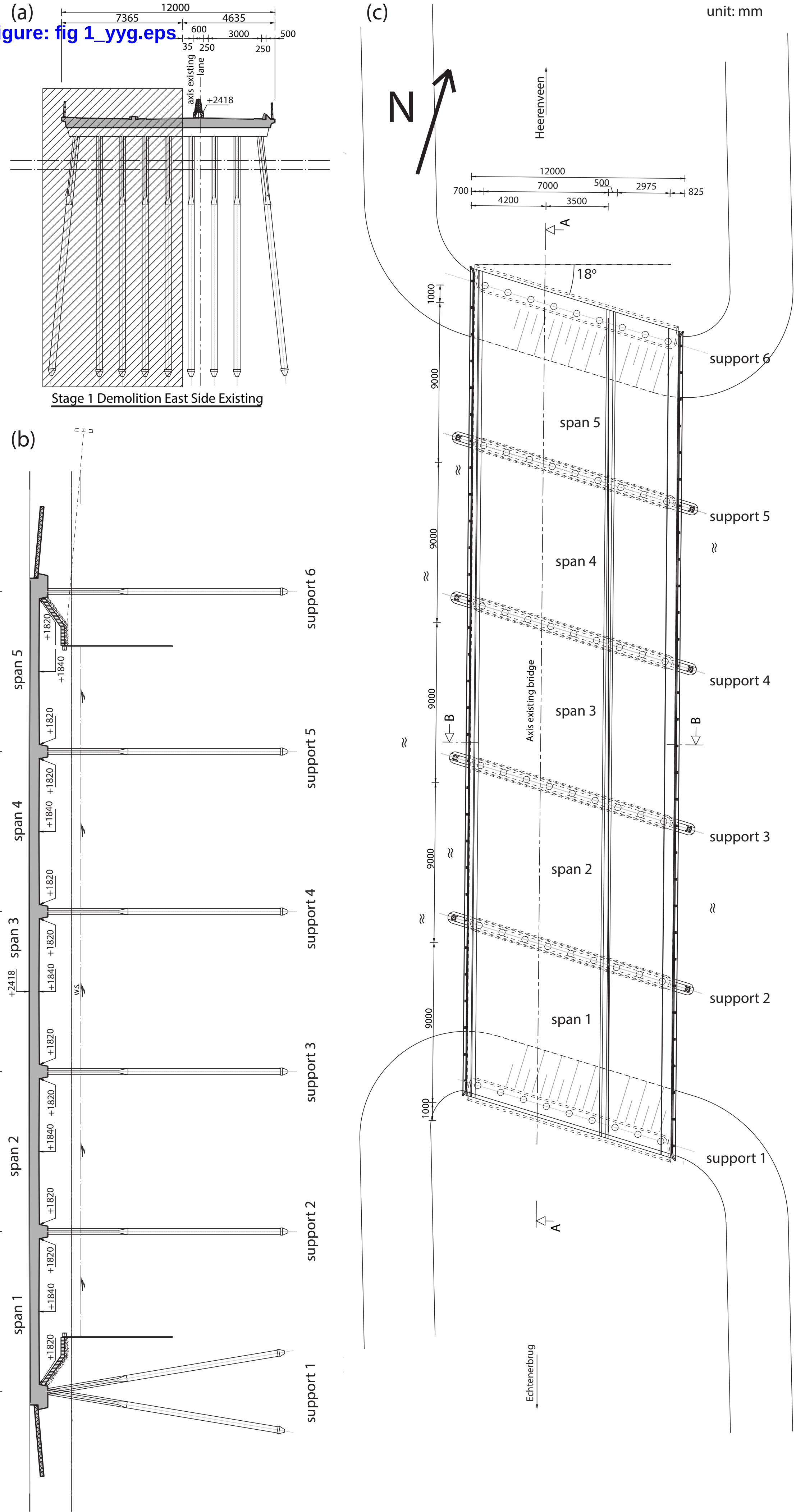

Figure 2
Click here to download Figure: fig 2_yyg.eps

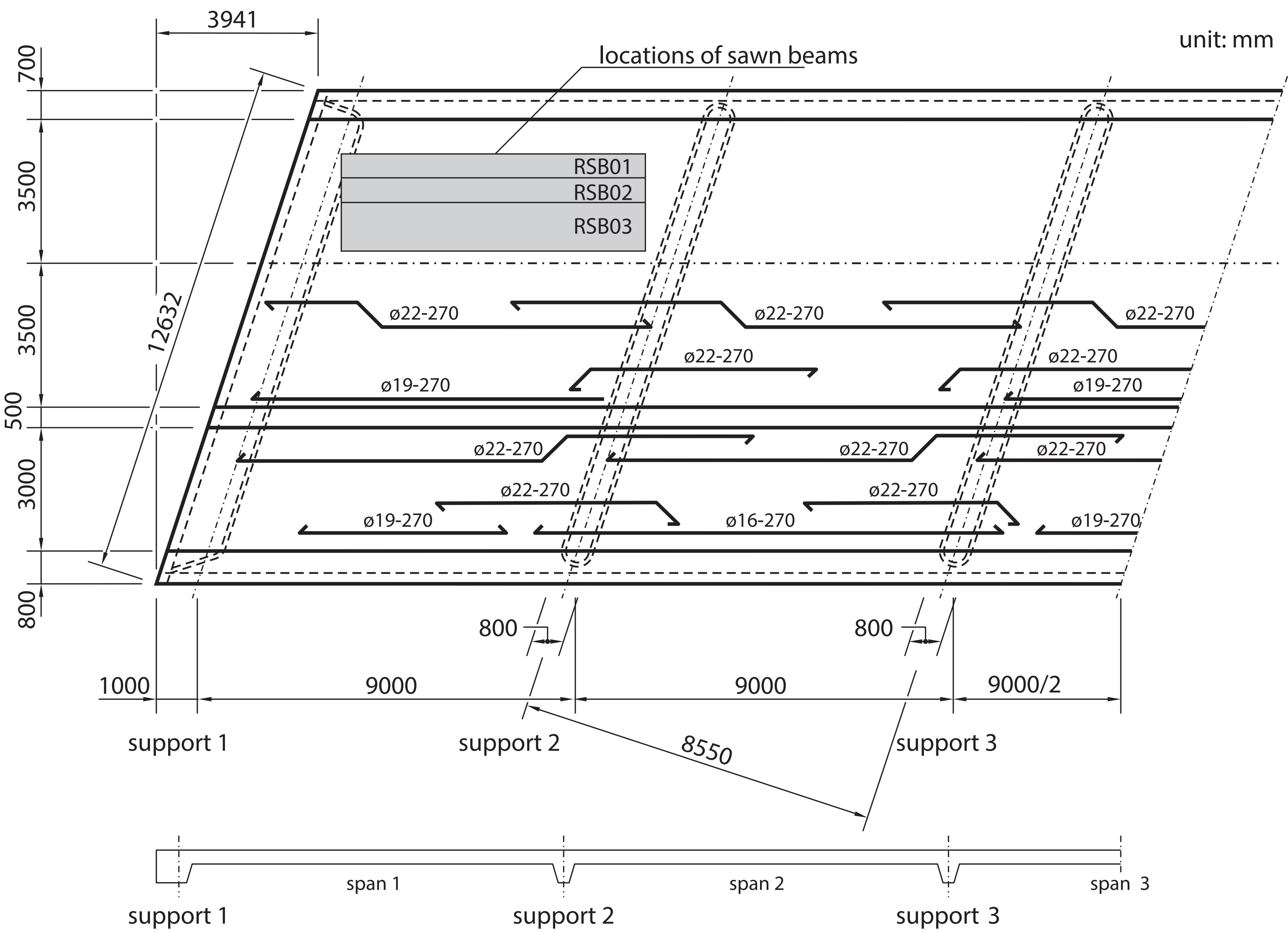

Figure 3
Click here to download Figure: fig 3.eps

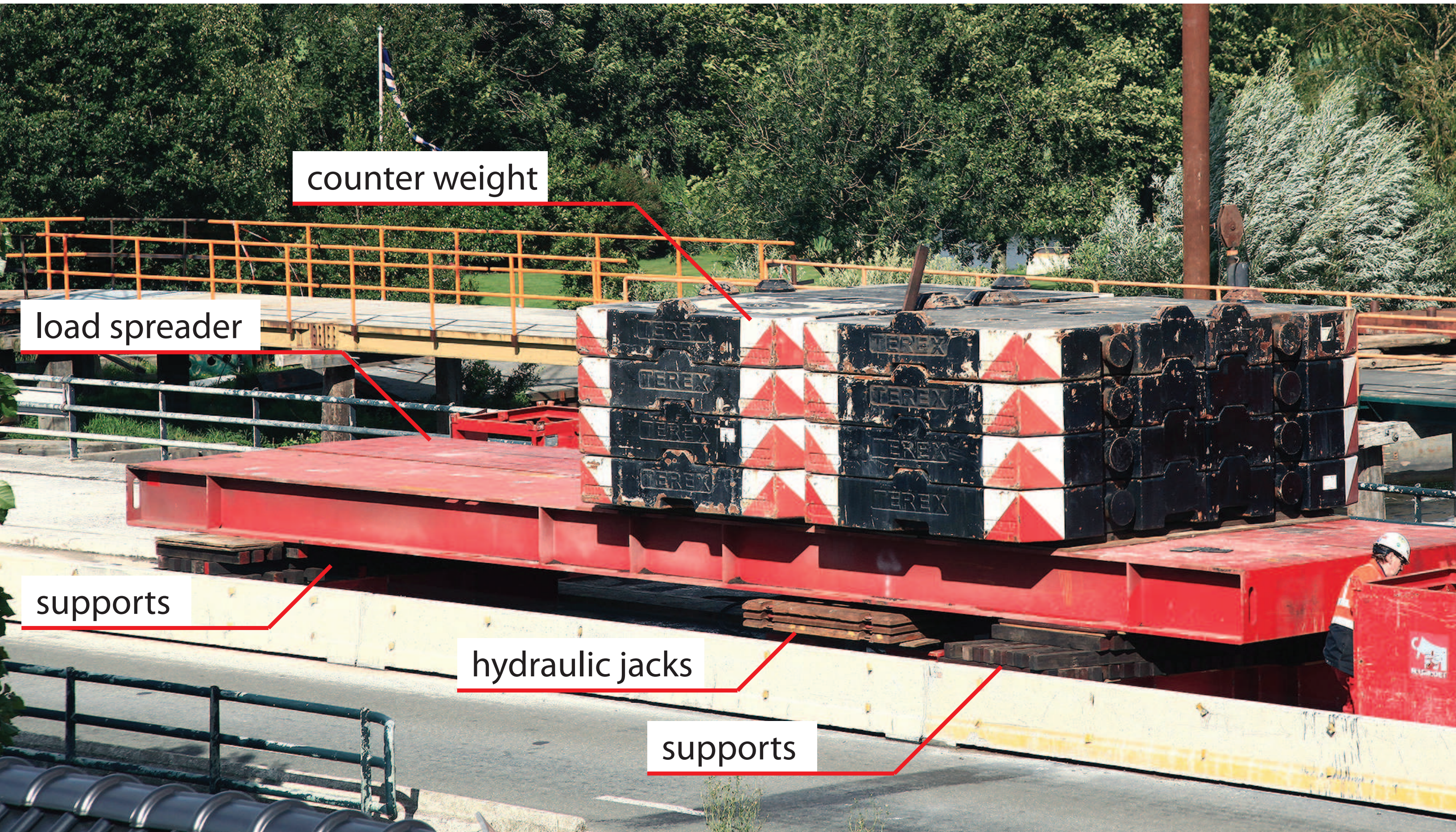

Figure 4
Click here to download Figure: fig 4_yyg.eps

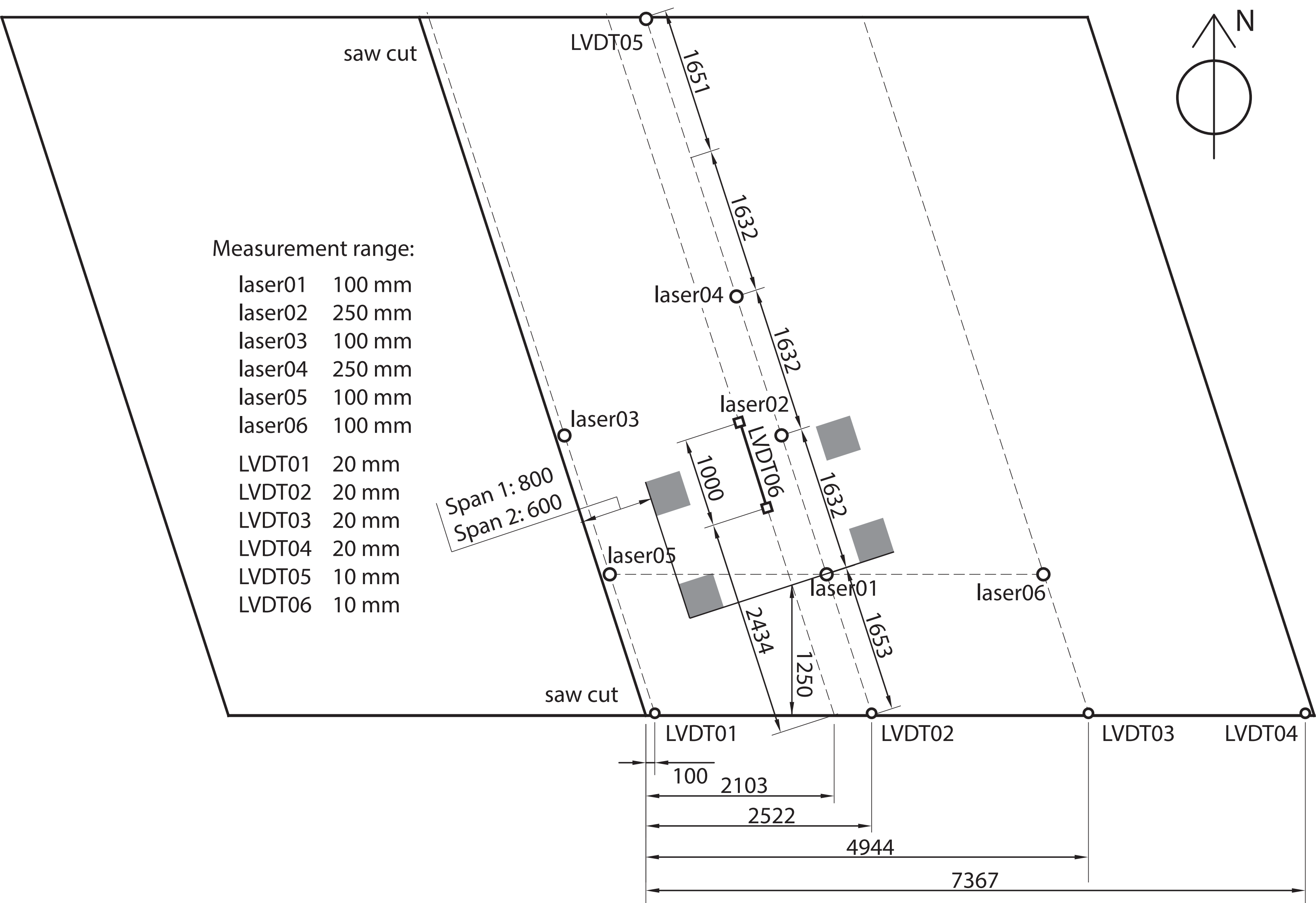

Figure 5
Click here to download Figure: fig 5_yyg.eps

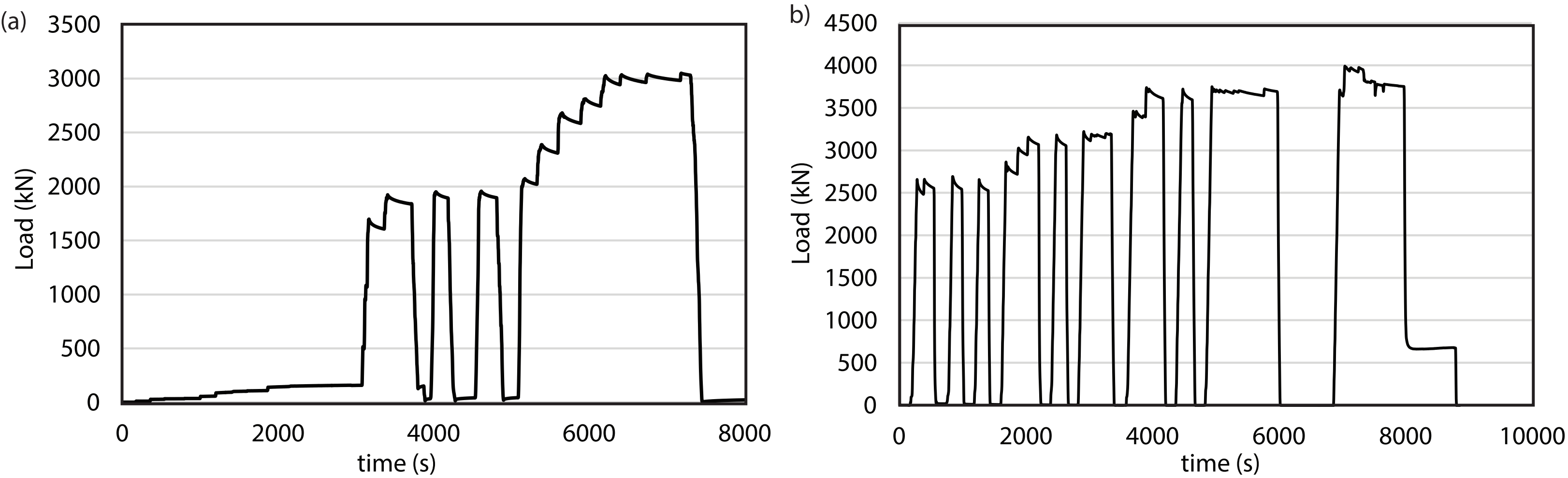

Figure 6
Click here to download Figure: fig 6_yyg.eps

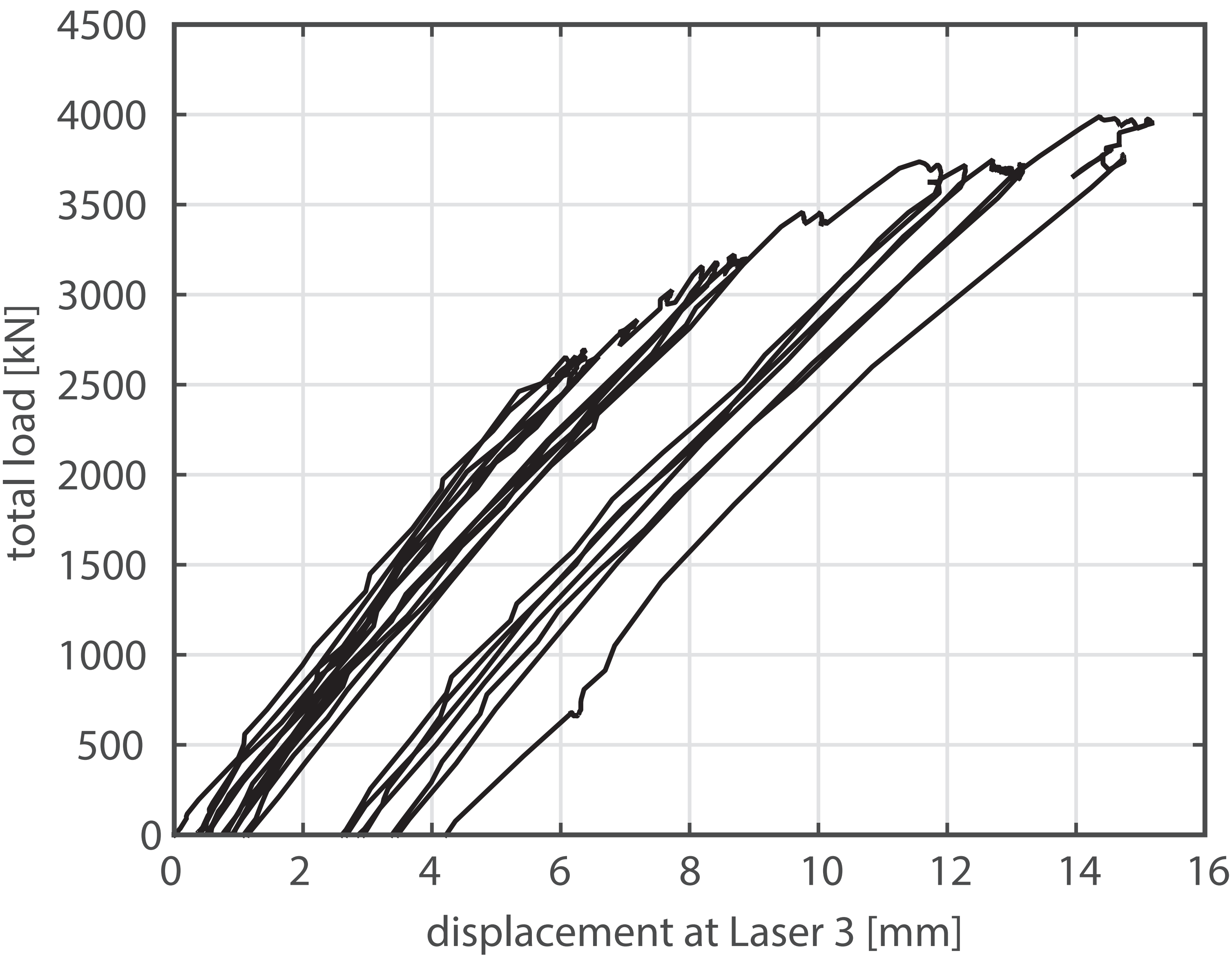

Figure 7
Click here to download Figure: fig 7.eps

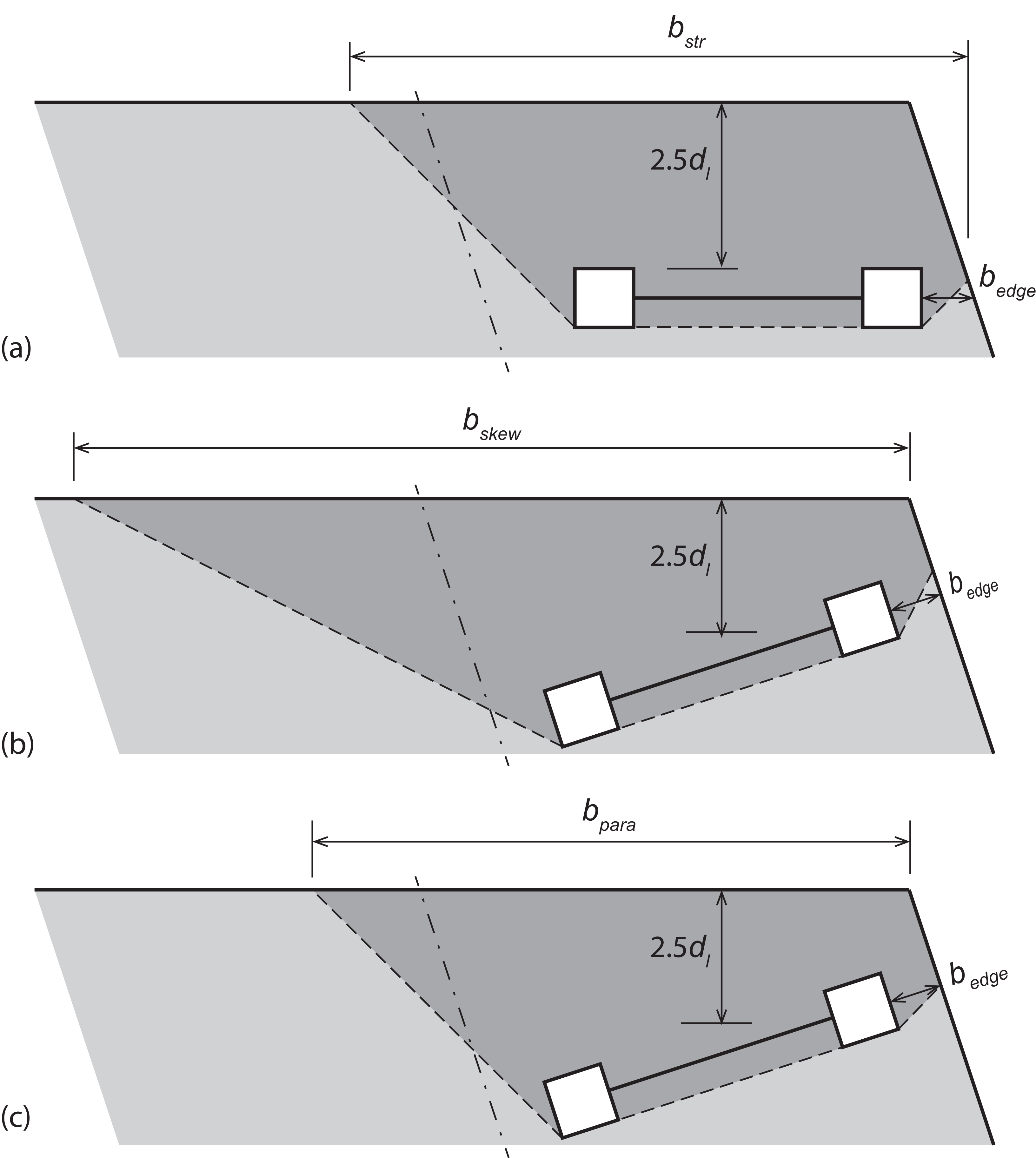

Figure 8
Click here to download Figure: fig 8_yyg.eps

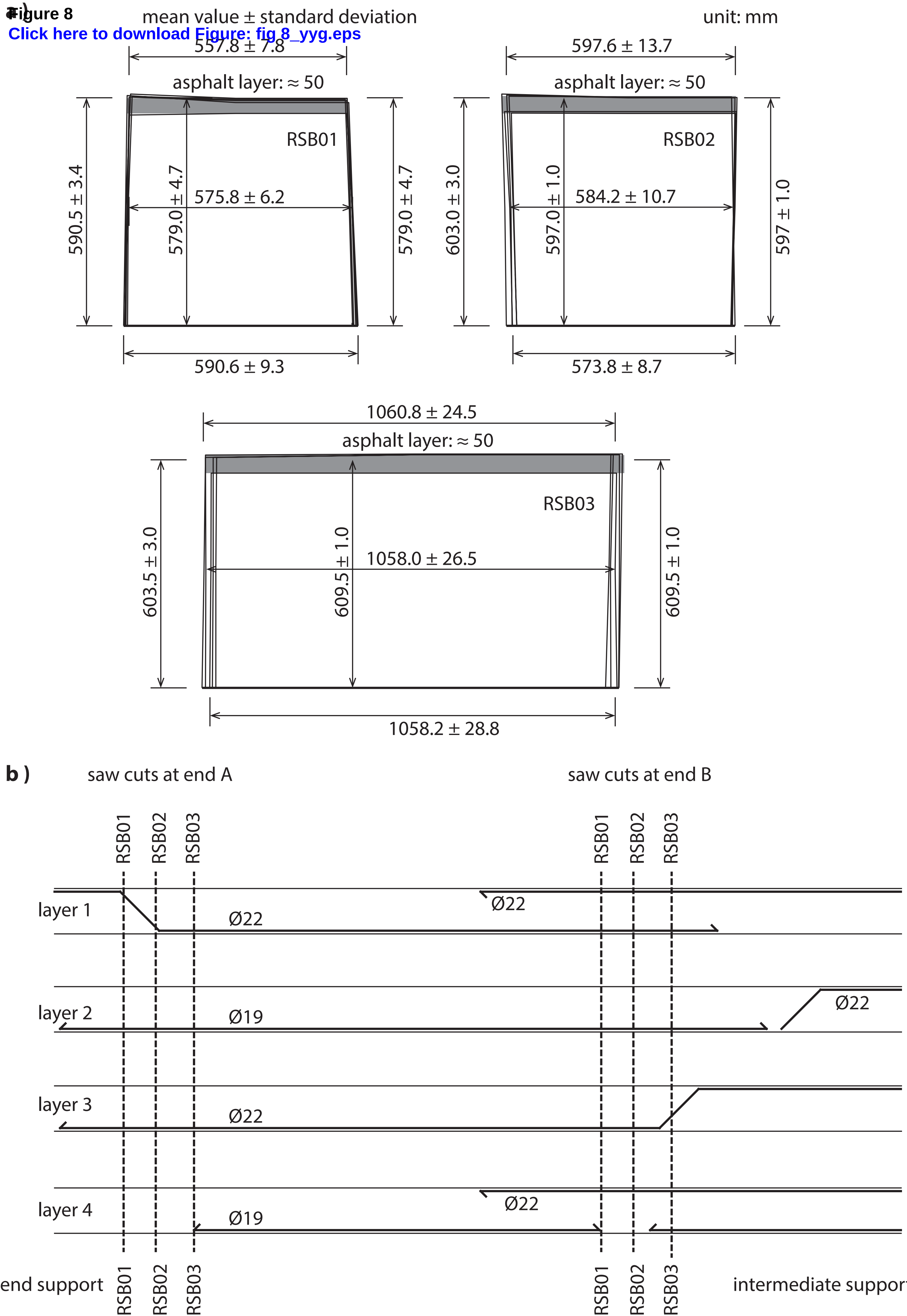

Figure 9
Click here to download Figure: fig 9_yyg.eps

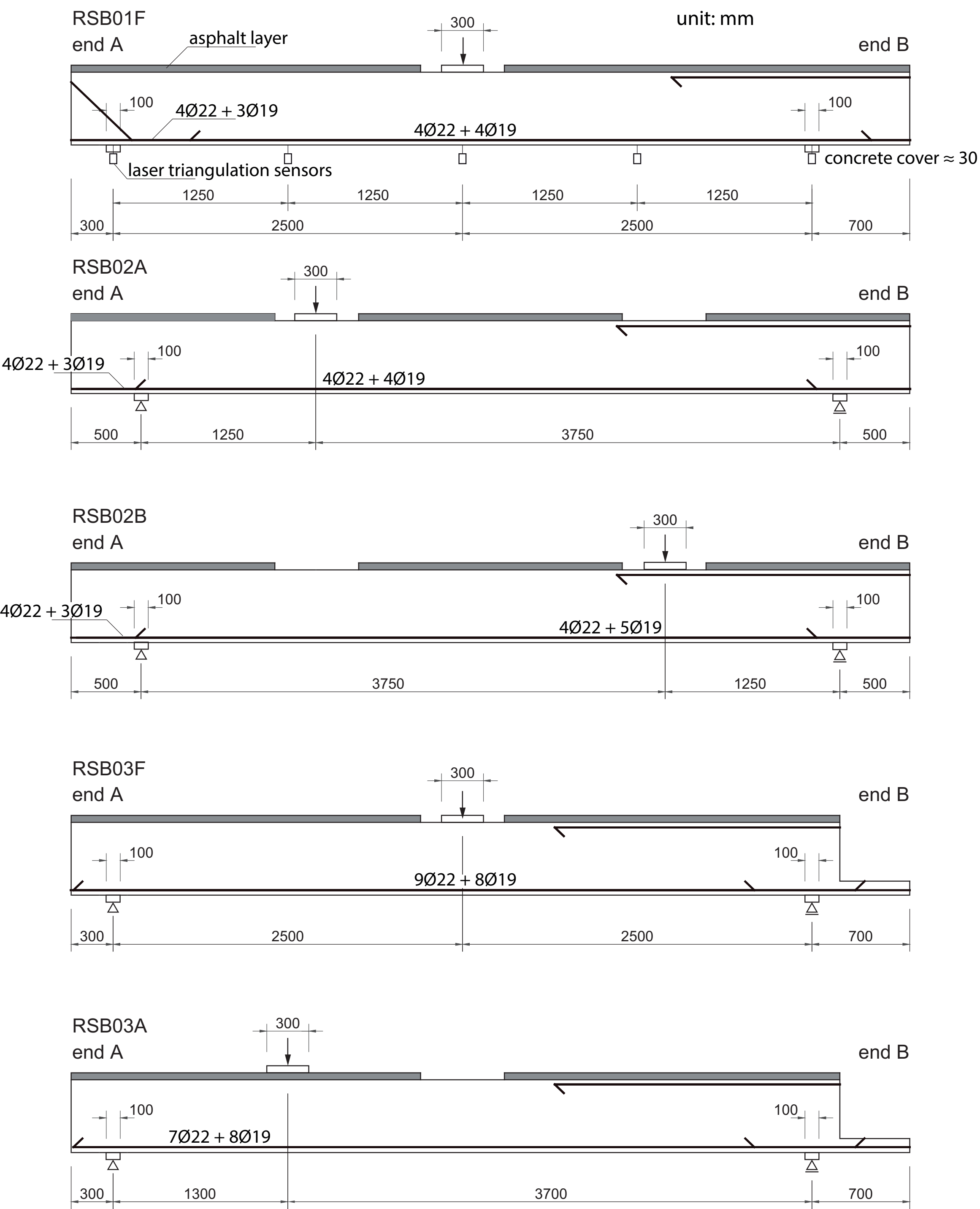

Figure 10
Click here to download Figure: fig 10_yyg.eps

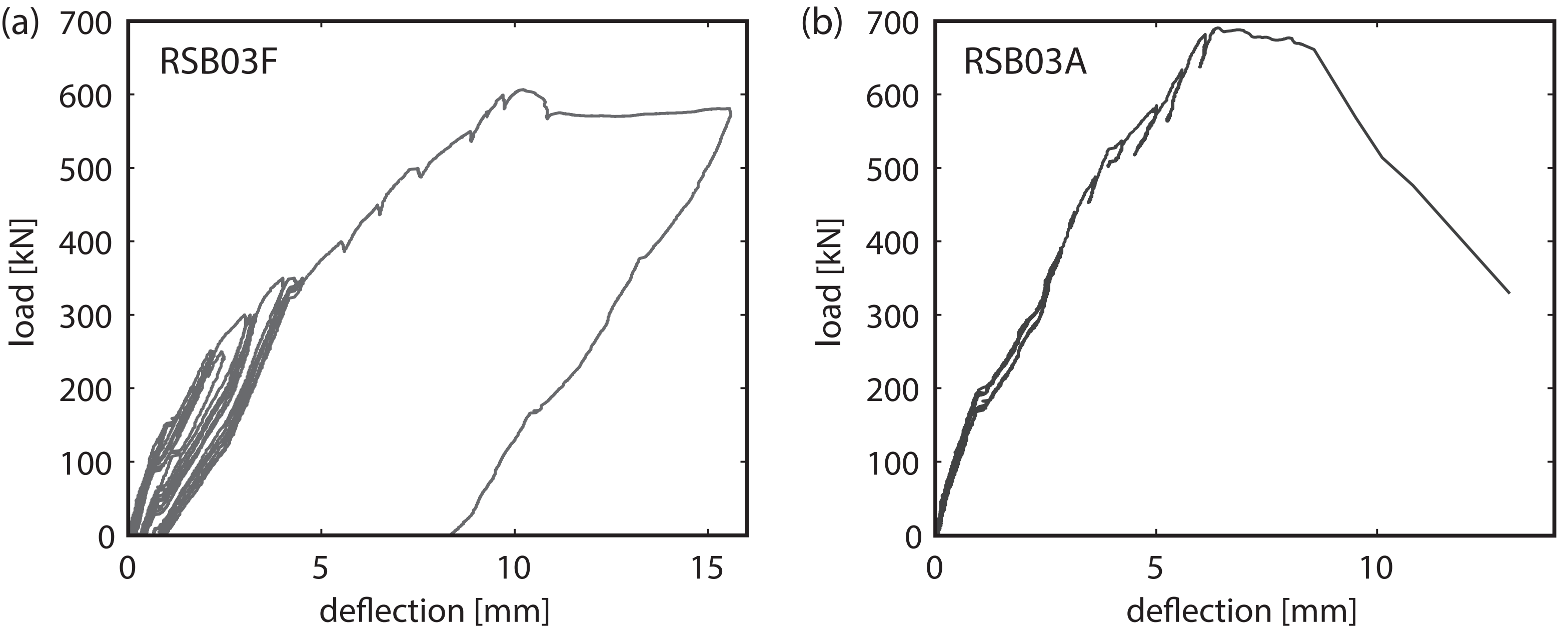

Figure 11
Click here to download Figure: fig 11.eps